Journal of Alloys and Compounds 509 (2011) 6359–6363

Contents lists available at ScienceDirect

Journal of Alloys and Compounds

journal homepage: www.elsevier.com/locate/jallcom

Complex permeability and microwave absorption properties of planar anisotropy $Ce_2Fe_{17}N_{3-\delta}$ particles

Wen-liang Zuo, Liang Qiao*, Xiao Chi, Tao Wang, Fa-shen Li*

Institute of Applied Magnetics, Key Laboratory of Magnetism and Magnetic Materials of the Ministry of Education, Lanzhou University, Lanzhou 730000, People's Republic of China

ARTICLE INFO

Article history:
Received 20 December 2010
Received in revised form 24 February 2011
Accepted 17 March 2011
Available online 29 March 2011

Keywords:
Intrinsic permeability
$Ce_2Fe_{17}N_{3-\delta}$
Effective medium theory
Planar anisotropy

ABSTRACT

The effective complex permeability of $Ce_2Fe_{17}N_{3-\delta}$ particles/epoxy resin composites with various volume concentrations p were measured in the frequency range of 0.1–15 GHz. The intrinsic quasi-static permeability $\mu'_{0,i}$ of $Ce_2Fe_{17}N_{3-\delta}$ particle was calculated by Bruggerman's (BG) effective medium theory. Meanwhile, the effective quasi-static permeability $\mu'_{0,e}$ of composites were calculated by the BG theory and modified Bruggerman's (MBG) effective medium theory, respectively. Through analyzing the experiment data, the effective shape factors of $Ce_2Fe_{17}N_{3-\delta}$ composites were determined. The intrinsic natural resonance frequency of $Ce_2Fe_{17}N_{3-\delta}$ was obtained using Landua–Lifshitz–Gilbert (LLG) equation. The minimum EM absorbing values with RL ≤ -30 dB are observed for all the volume concentrations.

1. Introduction

In recent years, with the growth in the utilization of communication and electronic devices such as mobile phone, intelligent transport and satellite broadcast system in industrial, commercial and military applications, electromagnetic interference is becoming a serious problem. Many electromagnetic materials with high permeability at microwave frequency have been attracted much attentions. Resin composites of Spinel-type ferrite were often used as electromagnetic materials [1,2]. However, the permeability of Spinel-type ferrite decreased quickly in high frequency due to the Snoek's limit [3]. In order to remain high permeability at higher frequency, a good method is using the materials with planar anisotropy. Generally, the product of the static permeability and the resonance frequency of the magnetic materials with planar anisotropy satisfies the equation [4]:

$$(\mu_s - 1)f_r = \frac{\gamma}{2\pi}\sqrt{\frac{H_\theta}{H_\varphi}}M_s, \quad (1)$$

where γ is the gyromagnetic ratio; M_s is the saturation magnetization; H_θ and H_φ are the out-of-plane and in-plane anisotropy fields, respectively. Therefore, larger initial permeability and higher resonance frequency can be achieved as long as H_θ is larger than H_φ. For instance, planar anisotropy Co_2Z ferrite has smaller saturation magnetization (0.27 T) than $NiFe_2O_4$ spinel ferrites (0.34 T) but exhibits higher resonance frequency and larger initial permeability [4–7]. However, the low saturation magnetization of Co_2Z limits the further improvement of its high frequency properties.

$Ce_2Fe_{17}N_{3-\delta}$ is a typical ternary rare earth iron nitride with planar anisotropy and higher saturation magnetization than that of Co_2Z [8]. Its natural resonance frequency f_r can be predicted in higher frequency while the value of permeability $\mu'_{0,i}$ is still unaltered or higher. Many studies have reported that the quasi-static permeability $\mu'_{0,i}$ is 8–12 and the resonance frequency is 1.5 GHz for bulk Co_2Z [9–11]. In order to contrast with bulk Co_2Z, the intrinsic quasi-static permeability $\mu'_{0,i}$ and resonance frequency f_r of $Ce_2Fe_{17}N_{3-\delta}$ material should be known. However, the permeability and resonance frequency are varied for magnetic fillers with different volume concentration. Furthermore, the intrinsic permeability of the magnetic metallic particles cannot be measured directly due to the lack of appropriate techniques in high frequency range [12]. To obtain the intrinsic permeability of the magnetic metallic particle, many researches reported that the effective medium theory is a reasonable method to obtain the intrinsic permeability of magnetic fillers [13–16].

In this article, the intrinsic quasi-static permeability $\mu'_{0,i}$ of $Ce_2Fe_{17}N_{3-\delta}$ particles was obtained by using Bruggerman's (BG) effective medium theories. Meanwhile, the frequency dependent permeability of $Ce_2Fe_{17}N_{3-\delta}$ composites was simulated using the Landua–Lifshitz–Gilbert (LLG) equation. Through analyzing the result, we obtained the resonance frequency of $Ce_2Fe_{17}N_{3-\delta}$. Both the permeability and resonance frequency of $Ce_2Fe_{17}N_{3-\delta}$ are larger than that of bulk Co_2Z. Therefore, $Ce_2Fe_{17}N_{3-\delta}$ material with high saturation magnetization and planar anisotropy is a promising candidate for electromagnetic material working in the higher frequency range.

* Corresponding authors. Tel.: +86 0931 8914171; fax: +86 0931 8914160.
E-mail addresses: qiaoliang@lzu.edu.cn (L. Qiao), lifs@lzu.edu.cn (F.-s. Li).

0925-8388/$ – see front matter © 2011 Elsevier B.V. All rights reserved.
doi:10.1016/j.jallcom.2011.03.105

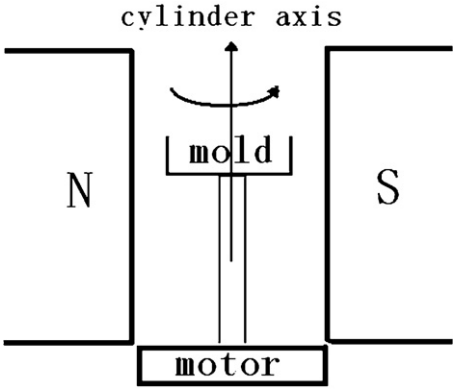

Fig. 1. The sketch of alignment device.

2. Effective medium theory

The general effective medium theory is based on the assumption that the magnetic particles are embedded in a host medium. The Maxwall–Garnett (MG) and Bruggeman (BG) effective medium theories are the most widely mixing theories [17,18]. However, MG effective medium theory is useful when the volume fraction of magnetic particles is either small or large [19]. The BG formula is

$$p\frac{\mu_i-\mu_e}{\mu_i+2\mu_e}+(1-p)\frac{\mu_m-\mu_e}{\mu_m+2\mu_e}=0, \quad (2)$$

where p is the volume fraction of magnetic particles; μ_i is the intrinsic permeability of magnetic particles; μ_e is the effective permeability of composites; μ_m is the permeability of medium ($\mu_m = 1$ for the epoxy resin in this work). The formula is valid when the particles are spherical and the radius is smaller than skin depth. For the irregular shape of inclusions, the modified BG (MBG) formula becomes:

$$p\frac{\mu_i-\mu_e}{\mu_e+n_0(\mu_i-\mu_e)}=(1-p)\frac{(\mu_e-\mu_m)}{\mu_e+n_0(\mu_m-\mu_e)}, \quad (3)$$

where n_0 is the shape factor (effective demagnetization factor) of inclusions, and it is customarily used as a fitting parameter to provide an agreement with measured data [16,20]. However, the conclusion was not supported by many experiments [21–23].

3. Experimental

The alloy Ce_2Fe_{17} ingots were prepared from Ce (>99.9% in purity), Fe (>99.99% in purity) by arc-melting under Ar atmosphere. Extra 5% Ce was added for compensating the loss of Ce due to evaporation. The ingots were remelted three times to ensure homogeneity and then annealed at 1273 K for 168 h under vacuum. The annealed ingots were then milled for 8 h by a planetary-type apparatus (QM-1F) with a ball-to-powder weight ratio of 20:1 in hexane. The nitrogenation reaction of the ball-milled particles was performed in a stainless steel tube (pressure: 1 bar, volume: about 1000 cm^3) with high-purity nitrogen gas (typically 5N5) for 2 h at 500 °C.

The aligned sample was prepared by mixing the $Ce_2Fe_{17}N_{3-\delta}$ particles with epoxy resin. The composite was then put into a non-magnetic cylinder mold. The sketch of the alignment device was shown in Fig. 1. It can be seen that the mold is connected with a motor which enables the mold to rotate in a static magnetic field, in which the cylinder axis is perpendicular to the field. This process ensures that the basal planes of $Ce_2Fe_{17}N_{3-\delta}$ particles were aligned parallel to each other and c-axis was parallel to the axis of the cylinder. The epoxy resin composites for measurement of complex permeability were prepared by mixing the $Ce_2Fe_{17}N_{3-\delta}$ particles with epoxy resin and pressing into a toroidal shape ($\emptyset_{out}$ = 7.00 mm, $\emptyset_{in}$ = 3.04 mm).

The phases were examined by X-ray diffraction (XRD, Philips X'perts) using Cu K_α radiation. The morphology was analyzed by scanning electron microscope (SEM) (HITACHI S-4800). Magnetic properties were characterized using a vibrating sample magnetometer (VSM, Lakeshore 7304, USA). The accurate volume concentrations were corrected by comparing M_s of composites with $Ce_2Fe_{17}N_{3-\delta}$ particles. The complex permeability of the composite samples was obtained using an Agilent E8363B vector network analyzer in the 0.1–15 GHz range.

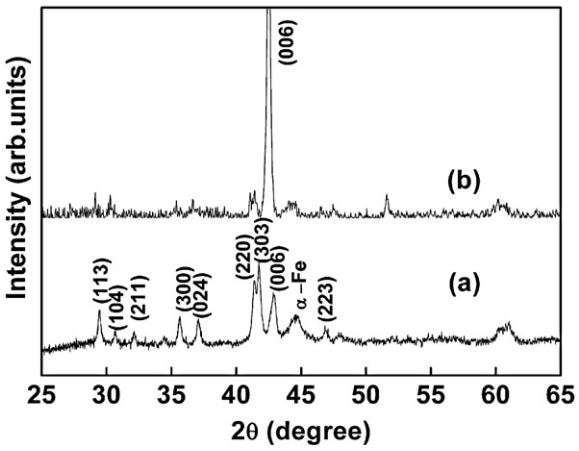

Fig. 2. (a) X-ray diffraction pattern of $Ce_2Fe_{17}N_{3-\delta}$ particles; (b) aligned $Ce_2Fe_{17}N_{3-\delta}$ composite.

4. Results and discussion

4.1. Microstructure and static magnetic properties

Fig. 2(a) shows the X-ray diffraction pattern measured on the random aligned $Ce_2Fe_{17}N_{3-\delta}$ particles which have a rhombohedral Th_2Zn_{17}-type structure. It is found that the powders are almost single phase except for a few α-Fe. The X-ray diffraction pattern of aligned $Ce_2Fe_{17}N_{3-\delta}$ composite is shown in Fig. 2(b). It is found that the intensity of the (hk0) crystalline plane reflection increases dramatically, whereas the intensity of other reflections almost vanishes. As compare to the isotropic $Ce_2Fe_{17}N_{3-\delta}$, this result indicates that the easy magnetization directions were in the c-plane for the $Ce_2Fe_{17}N_{3-\delta}$ particles. Scanning electron microscopy images reveal that the particles are irregular shape and are about 2–4 μm in size, as shown in Fig. 3.

The magnetic hysteresis loops of samples were measured by a vibrating sample magnetometer under room temperature at the field from −1.2 T to 1.2 T. The results are listed in Table 1. From the M_s of composites, we calculated the accurate volume fraction of $Ce_2Fe_{17}N_{3-\delta}$ composites and it changes from 29.0% to 61.3%.

4.2. Complex permittivity and permeability

The real part ε' and imaginary part ε'' of complex permittivity are almost independent of frequency in the frequency

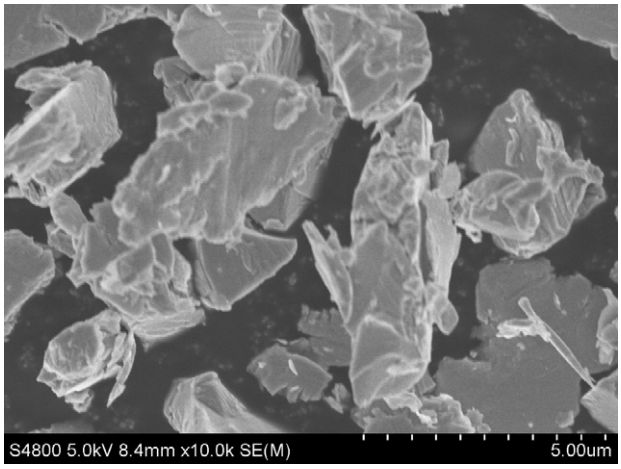

Fig. 3. The SEM images of $Ce_2Fe_{17}N_{3-\delta}$ particles.

Table 1
The static magnetic properties and effective shape factors of $Ce_2Fe_{17}N_{3-\delta}$ composites with various volume concentrations p.

Volume concentrations p	M_s (emu/g)	H_c (Oe)	Effective shape factor	
			N (Ref. [21])	n_0 (this work)
29.0%	111.4	62	0.241	0.204
46.2%	127.9	61	0.279	0.268
51.3%	131.1	60	0.292	0.333
53.9%	132.5	60	0.311	0.352
61.3%	136.1	60	0.333	0.415
100%	147.5	53	–	–

range of 0.1–15 GHz. ε' is around 16, 36, 30, 35, and 27 for volume concentrations of 29.0%, 46.2%, 51.3%, 53.9%, and 61.3%, respectively. ε'' is about 2.5 for all composites. The frequency dependence of the real part μ' and the imaginary part μ'' of permeability for the $Ce_2Fe_{17}N_{3-\delta}$ composites with various volume concentrations p are shown in Fig. 4. The effective quasi-static permeability $\mu'_{0,e}$ of composites is defined as the real part of permeability at 0.1 GHz. The effective resonance frequency $f_{r,e}$ is defined as the corresponding frequency for the maximum imaginary part of permeability. It can be seen that the $\mu'_{0,e}$ of composites increases from 3.04 to 5.73 with the increase of volume concentration. However, due to the demagnetizing field effect, the $f_{r,e}$ of composites decreases from 9.6 GHz to 3.0 GHz with the increase of volume concentration [21,24]. Many experiments reported that the BG theory is valid for the concentration of 50 vol.% [19,25]. Therefore, the quasi-static intrinsic permeability $\mu'_{0,i}$ of $Ce_2Fe_{17}N_{3-\delta}$ is calculated

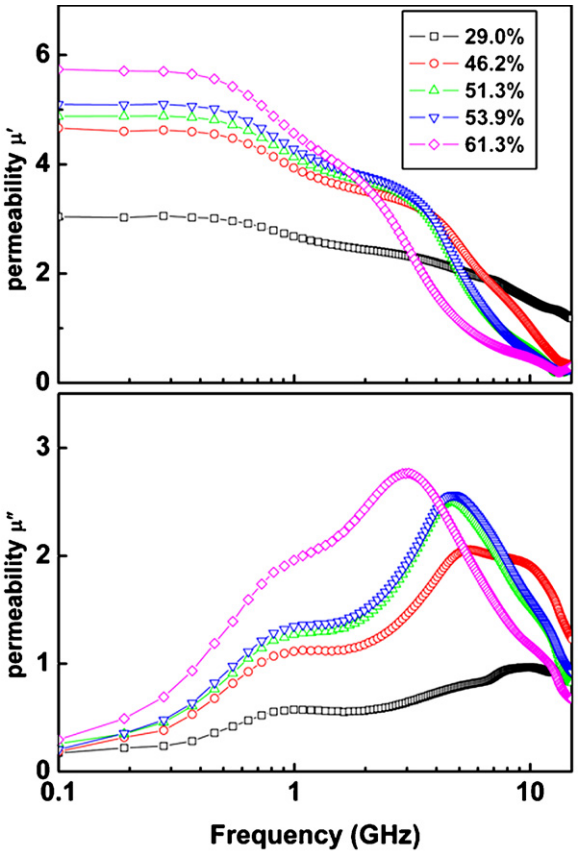

Fig. 4. The frequency dependence of the real part μ' and the imaginary part μ'' of permeability for the $Ce_2Fe_{17}N_{3-\delta}$ composites with various volume concentrations.

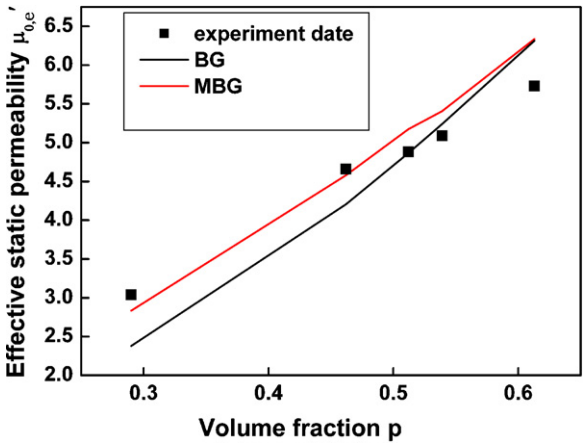

Fig. 5. The effective quasi-static permeability dependence on p for $Ce_2Fe_{17}N_{3-\delta}$ composites. The squares are experimental data; the black line and red line are the calculated data based on Eqs. (2) and (3), respectively. (For interpretation of the references to color in text, the reader is referred to the web version of the article.)

by using Eq. (2) with the sample of $p = 51.3\%$. To research the validity of quasi-static intrinsic permeability, the effective quasi-static permeability was calculated using Eqs. (2) and (3), respectively, and the parameter of the shape factors n_0 obtained from this work in Eq. (3) [21]. The results are shown in Fig. 5. It can be seen that the disagreement between calculated and measured $\mu'_{0,e}$ is clear for both the high and low volume fraction for the BG theory. The phenomenon can be attributed to the aggregation of inclusions. It is known that the aggregation is not considered in BG theory whereas it is inevitable during the particle mixing process. For the MBG theory, the calculated and measured data agree well for the low volume fractions. However, for high volume fractions, the disagreement is also obvious. In order to obtain the effective shape factors n_0 which is suited for our samples, we calculated the n_0 using Eq. (3) with the parameter of p and $\mu'_{0,e}$ obtained from experiment data and the quasi-static intrinsic permeability from above calculation. The results are listed in Table 1. It is found that the n_0 increases with the increase of volume concentration. This behavior is also observed by other researches [21–23]. However, comparing with the shape factor from this work [21], the n_0 is smaller at lower volume concentration (smaller than 51.3 vol.%) and larger at higher volume concentration (higher than 51.3 vol.%). This discrepancy might be attributed to the irregular shape of the particles. It is known that the aggregation is more easily for the irregular particles than that of spherical shape. At the low volume concentration, the particles tend to form small chainlike aggregates (the demagnetization factor is less than 1/3). On the contrary, at the high volume concentration, the aggregation tend to become spherical (the demagnetization factor equal to 1/3) and flake-like aggregation (the demagnetization factor is possible larger than 1/3) [21,23]. Therefore, the quasi-static intrinsic permeability is reasonable to obtain from above calculation and the value is 12.5. Obviously, $Ce_2Fe_{17}N_{3-\delta}$ materials with planar anisotropy and high saturation magnetization show the larger permeability than that of bulk Co_2Z.

4.3. Natural resonance frequency

For the particle composites, the resonance frequency is determined by magnetocrystalline anisotropy energy and demagnetizing energy. However, the intrinsic natural resonance frequency of bulk materials should only be determined by its magnetocrystalline anisotropy energy. It is known that when the particle

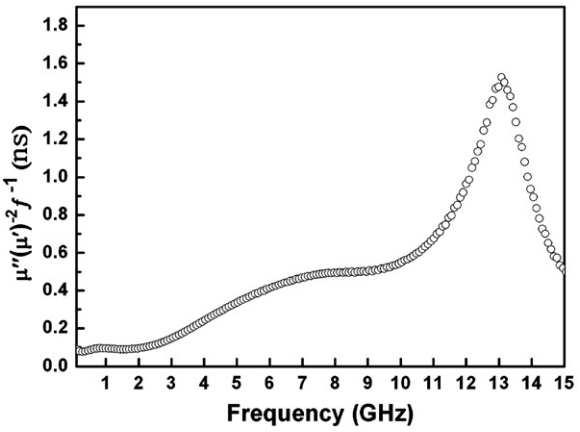

Fig. 6. The values of $\mu''(\mu')^{-2}f^{-1}$ for the $Ce_2Fe_{17}N_{3-\delta}$ composites with 51.3 vol.% vs frequency.

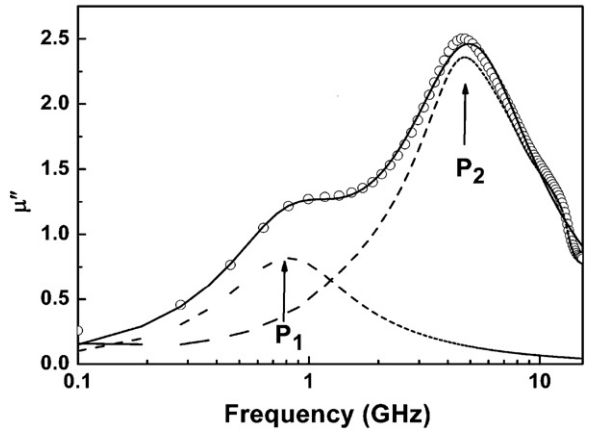

Fig. 7. The imaginary part μ'' of permeability for the $Ce_2Fe_{17}N_{3-\delta}$ composites with 51.3 vol.%; the dashed lines of P_1 and P_2 are the fitted resonance peaks for the first and second peaks, respectively; the real lines is the linear overlap of P_1 and P_2.

is spherical and the interactions of inclusions are ignored, the demagnetizing energy has no contribution to the resonance frequency [22]. This also means that the effective shape factor n_0 for the particle composites should be 1/3. In order to discuss the mechanism of natural resonance, we should use the sample with volume concentration of 51.3% which has the effective shape factor about 1/3.

In general, the microwave magnetic loss of magnetic materials originates mainly from hysteresis, domain wall resonance, eddy current loss, and natural ferromagnetic resonance. The hysteresis loss is mainly caused by the time lags of the magnetization vector behind the external electromagnetic field vector and is negligible in a weak applied field. The domain wall resonance usually occurs only in the 1–100 MHz range. The eddy current loss contribution to the imaginary part permeability is related to the thickness (d) and the electric conductivity (σ) [26–29]:

$$\mu''(\mu')f^{-1} = \frac{2}{3}\pi\mu_0 d^2\sigma, \tag{4}$$

where μ_0 is the permeability of vacuum. If the magnetic loss only results from eddy current, the values of left-hand side of Eq. (4) should be constant when frequency is varied. We call this the skin-effect criterion. Fig. 6 shows the values of $\mu''(\mu)^{-2}f^{-1}$ for the $Ce_2Fe_{17}N_{3-\delta}$ composite with 51.3 vol.%. As we can see, the change extent is larger than 1.5 ns. Thus, the magnetic loss in $Ce_2Fe_{17}N_{3-\delta}$ composites is mainly caused by the natural resonance. For the natural resonance mechanism, the complex permeability spectra can be fitted by using the Landua-Lifshitz-Gilbert (LLG) equation [28–30]:

$$\mu'' = \sum_i^n \chi'_i \frac{(f/f_i)\alpha(1+(f/f_i)^2(1+\alpha^2))}{(1-(f/f_i)^2(1+\alpha^2))^2 + 4\alpha^2(f/f_i)^2}, \tag{5}$$

where n is the number of peaks (n = 2 in this work); χ'_i is the initial susceptibilities; f is the frequency; f_i is the spin resonance frequency (intrinsic natural resonance frequency of composites); α is the damping coefficient. The typical curve-fitting results for the $Ce_2Fe_{17}N_{3-\delta}$ composites with 51.3 vol.% are shown in Fig. 7. The fitting resonance frequencies f_i are 1.2 and 7.3 GHz. Damping coefficients are 0.99 and 1.04, respectively. It is known that the magnetocrystalline anisotropy field of α-Fe is 600 Oe [14], so the natural resonance frequency $f_r = \gamma H_0$ = 1.68 GHz. This is close to the fitting data of the first weak peak P_1 in the spectrum. Therefore, the first resonance peak is come from the natural resonance of α-Fe. For polycrystalline $Ce_2Fe_{17}N_{3-\delta}$ material, Eq. (1) can be disassembled as follows [4,22]:

$$f_r = \frac{\gamma}{2\pi}\sqrt{H_\theta H_\varphi}, \tag{6}$$

$$\mu_s - 1 = \frac{M_s}{2H_\varphi}, \tag{7}$$

Therefore, the based plane anisotropy field H_φ of $Ce_2Fe_{17}N_{3-\delta}$ can be calculated and is 0.061 T. The out-of-plane anisotropy fields H_θ of $Ce_2Fe_{17}N_{3-\delta}$ is about 2 T [31]. Theoretical calculation of natural resonance frequency should be 9.7 GHz, which is close to the fitting data of the second peak (7.3 GHz). Therefore, the second peak is the natural resonance of $Ce_2Fe_{17}N_{3-\delta}$. The calculated product of the static permeability and the resonance frequency is 84 GHz, which is larger than the value of conventional Snoek's limit $2\gamma M_s/3$ = 27 GHz. Therefore, planar anisotropy $Ce_2Fe_{17}N_{3-\delta}$ material can overcome Snoek's limit and achieve higher initial permeability at higher frequency.

4.4. Microwave absorbing properties

The reflection loss (RL) of EM wave is determined according to the following equations:

$$\mathrm{RL(dB)} = 20\log_{10}\left|\frac{Z_{in}-Z_0}{Z_{in}+Z_0}\right|, \tag{8}$$

$$\frac{Z_{in}}{Z_0} = \sqrt{\frac{\mu}{\varepsilon}}\tanh\left[j\frac{2\pi ft}{c}\sqrt{\mu\varepsilon}\right]. \tag{9}$$

where Z_{in} is the impedance of the composites, Z_0 is the intrinsic impedance of free space, c is the velocity of light in free space, t is the thickness of composite, f is the frequency of the incident EM wave, $\mu = \mu' - j\mu''$ is the complex permeability and $\varepsilon = \varepsilon' - j\varepsilon''$ is the complex permittivity.

Fig. 8 shows the frequency dependence of the calculated RL for the $Ce_2Fe_{17}N_{3-\delta}$ composite with various volume concentrations p. It can be seen that the EM absorbing values with RL ≤ −30 dB are observed for all the volume concentrations. In addition, $Ce_2Fe_{17}N_{3-\delta}$ composites have smaller matching thickness compared with Co_2Z composites at the same frequency [9]. That is attributed to the larger complex permeability of $Ce_2Fe_{17}N_{3-\delta}$ composite [9,32,33]. Therefore, $Ce_2Fe_{17}N_{3-\delta}$ material with high saturation magnetization and planar anisotropy may become a new electromagnetic material working with small thickness working in high frequency range.

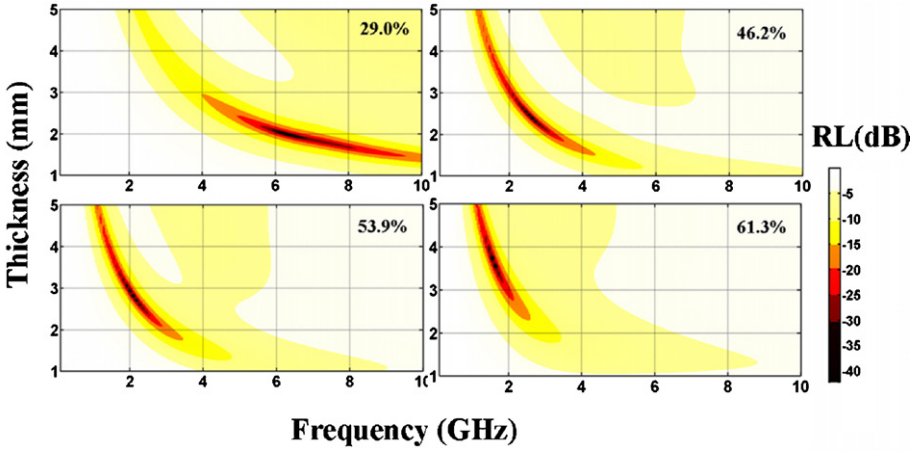

Fig. 8. The frequency dependence of the calculated RL for the $Ce_2Fe_{17}N_{3-\delta}$ composite with various volume concentrations.

5. Conclusions

The effective complex permeability of $Ce_2Fe_{17}N_{3-\delta}$ composites with various volume concentrations were measured in the frequency range of 0.1–15 GHz. The quasi-static intrinsic permeability $\mu'_{0,i}$ of $Ce_2Fe_{17}N_{3-\delta}$ material was calculated by effective medium theories and the value was 12.5. We use the skin-effect criterion to find that the magnetic loss is mainly caused by natural resonance. The resonance spectrum is simulated by using the LLG equation. The fitting natural resonance frequency of $Ce_2Fe_{17}N_{3-\delta}$ material was 7.3 GHz. Obviously, Both the quasi-static intrinsic permeability and natural resonance frequency are larger than that of bulk Co_2Z. The EM absorbing values RL ≤ -30 dB are observed for all the volume concentrations. Furthermore, $Ce_2Fe_{17}N_{3-\delta}$ composites have smaller matching thickness compared with Co_2Z composites at the same frequency. Therefore, $Ce_2Fe_{17}N_{3-\delta}$ material with high saturation magnetization and planar anisotropy may become a new electromagnetic material with small thickness working in high frequency range.

Acknowledgements

Authors wish to thank Physics Department of Lanzhou University for the SEM images of the samples. This work is supported by National Natural Science foundations of China (grant no. 10774061) and defense industrial technology development program (grant no. A142008174).

References

[1] Y. Naito, K. Suetake, IEEE Trans. Micro 19 (1971) 65–72.
[2] D.Y. Kim, Y.C. Chung, T.W. Kang, H.C. Kim, IEEE Trans. Magn. 32 (1996) 555–558.
[3] J.L. Snoek, Physica 14 (1948) 207–217.
[4] D.S. Xue, F.S. Li, X.L. Fan, F.S. Wen, Chin. Phys. Lett. 25 (2008) 4120–4123.
[5] T. Tsushima, T. Teranishi, K. Ohta, in: S. Chikazumi, et al. (Eds.), Handbook on Magnetic Substances, 9.2, 1975, p. 612, Table 9.3.
[6] G.H. Jonker, Philips Tech. Rev. 18 (1956) 145.
[7] K.N. Rozanov, Z.W. Li, L.F. Chen, J. Appl. Phys. 97 (2005) 013905.
[8] M.Q. Huang, Y. Zheng, K. Miller, J.M. Elbicki, S.G. Sankar, W.E. Wallace, R. Obermyer, J. Magn. Magn. Mater. 102 (1991) 91–95.
[9] Z.W. Li, G.Q. Lin, L.B. Kong, IEEE Trans. Magn. 44 (2008) 2255–2261.
[10] O. Kimura, M. Matsumoto, M. Sakakura, J. Am. Ceram. Soc. 78 (1995) 2857–2860.
[11] T. Nakamura, E. Hankui, J. Magn. Magn. Mater. 257 (2003) 158–164.
[12] W.M. Merrill, R.E. Diaz, M.M. LoRe, M.C. Squires, N.G. Alexopoulos, IEEE Trans. Antennas Propag. 47 (1999) 142–148.
[13] L. Olmedo, G. Chateau, C. Deleuze, J.L. Forveille, J. Appl. Phys. 73 (1993) 6692–6994.
[14] L.Z. Wu, J. ding, H.B. Jiang, C.P. Neo, J. Appl. Phys. 99 (2006) 083905.
[15] J.T. Jiang, L. Zhen, X.J. Wei, Y.X. Gong, W.Z. Shao, Y. Xu, K. He, J. Appl. Phys. 105 (2009), 07A526.
[16] K.N. Rozanov, A.V. Osipov, D.A. Petrov, S.N. Starostenko, E.P. Yelsukov, J. Magn. Magn. Mater. 321 (2009) 738–741.
[17] J.C.M. Garnett, Philos. Trans. R. Soc. London Ser. A 203 (1904) 385.
[18] D.A.G. Bruggeman, Ann. Phys. 416 (1935) 636.
[19] J.H. Paterson, R. Devine, A.D.R. Phelps, J. Magn. Magn. Mater. 196–197 (1999) 394–396.
[20] A.V. Osipov, K.N. Rozanov, N.A. Simonov, S.N. Starostenko, J. Phys. Condens. Matter 14 (2002) 9507–9523.
[21] A. Chevalier, M. Le Floch, J. Appl. Phys. 90 (2001) 3462–3465.
[22] Z.W. Li, Y.B. Gan, X. Xin, G.Q. Lin, J. Appl. Phys. 103 (2008) 073901.
[23] T. Tsutaoka, M. Ueshima, T. Tokunage, T. Nakamura, K. Hatakeyama, J. Appl. Phys. 78 (1995) 3983–3991.
[24] T. Nakamura, T. Tsutaoka, K. Hatakeyama, J. Magn. Magn. Mater. 137 (1994) 319–328.
[25] H.M. Musal Jr., H.T. Hahn, G.G. Bush, J. Appl. Phys. 63 (1988) 3768–3770.
[26] S.B. Liao, Ferromagnetic Physics (3), Science, Beijing, 2000, p. 17.
[27] M.Z. Wu, Y.D. Zhang, S. Hui, T.D. Xiao, S.H. Ge, W.A. Hines, J.I. Budnick, G.W. Taylor, Appl. Phys. Lett. 80 (2002) 4404–4406.
[28] L. Qiao, F.S. Wen, J.Q. Wei, J.B. Wang, F.S. Li, J. Appl. Phys. 103 (2008) 063903.
[29] F.S. Wen, H.B. Yi, L. Qiao, H. Zheng, D. Zhou, F.S. Li, Appl. Phys. Lett. 92 (2008) 042507.
[30] A. Aharoni, Introduction to the Theory of Ferromagntism, Clarendon, Oxford, 1996, p. 181 Chapter 8.
[31] X.C. Kou, F.R. de Boer, G. Chouteau, J. Appl. Phys. 83 (1998) 6899–6901.
[32] T. Inui, K. Konishi, K. Oda, IEEE Trans. Magn. 35 (1999) 3148–3150.
[33] A.R. Bueno, M.L. Gregori, M.C.S. Nobrega, J. Magn. Magn. Mater. 320 (2008) 846–870.